

A Parametric Analysis of Radiation Heat Transfer in Direct Injection Diesel Combustion

S.L. Chang, X.L. Yang and K.T. Rhee
Department of Mechanical and Aerospace Engineering
Rutgers, The State University of New Jersey
New Brunswick, New Jersey 08903

ABSTRACT

Radiation heat transfer in a direct injection-type diesel engine is investigated by a computational parametric analysis for various engine and combustion variables. A new model has been developed to compute the spectral radiation heat flux incident on various locations in the combustion chamber and to incorporate it with the spectral emissivity of the chamber wall surface. The model mainly differs from previous ones in several ways: (1) it uses the in-cylinder species distribution; (2) a new coordinate transformation method is introduced, instead of using geometric factors or the zonal method; (3) it computes the spectral volume absorptance of the combustion products through optical paths; (4) a new formulation and integration method are employed for the governing equation of radiation heat flux; etc. The main purpose of the present paper is to report some of results from a parametric analysis carried out by using the new computational model.

A NEW MODEL

A better modeling of radiation heat transfer is desired for a more comprehensive analysis of thermal loading of a diesel engine. A rigorous way of computing the radiation heat flux incident on a particular location of the combustion chamber wall will be implementing the equation of radiation heat transfer as accurately as possible. The equation calls for the detailed distributions of optical and thermal properties along individual optical paths in the hemispherical volume faced by the location. Several difficult issues remain to be overcome in achieving the above goals for a long time. They are the proper use of the in-cylinder species and temperature distributions in the modeling, the computation of optical and thermal properties of the species along the individual optical paths, the accurate implementation of the equation of monochromatic radiation heat transfer, to name a few. Each problem is discussed elsewhere by proposing the authors' solution. However, a brief description of the authors' methods for the individual problems are made in the following. Note that the main purpose of the present paper is to report results from a parametric analysis made in the present numerical method, which are not included in others.

In order to properly evaluate the space-resolved nature of the radiation heat transfer in diesel combustion, it is important to determine the instantaneous in-cylinder species and temperature distributions. It cannot be overemphasized that an assumption of uniform species distribution in diesel combustion is incapable of properly evaluating the spatial dependence of heat transfer. Such space-resolved distribution data, which may be found by using either experimental methods [1-3] or computational means, presently are not sufficient for an extensive analysis of the radiation process, in particular, for a parametric study of the process. As an alternative, a plume equation which seems to reasonably express the instantaneous species distribution has been introduced for radiation heat transfer analysis as [4],

$$f = f_0 \exp(-a\phi - b\phi^2 - cz^2) \quad (1)$$

where f represents the local burned fuel/air ratio or CO_2 or H_2O concentrations, etc., and f_0 , a , b , c are the ones to be respectively determined at each engine crank angle by using the above mentioned methods. For simplicity but perhaps as one of the only presently available alternatives, the burned fuel air ratio may be used for computing the instantaneous local temperature distribution [5]. The above plume equation enables one to choose plume geometries of varied species distributions. Therefore, the above equation can be used in a parametric analysis of radiation heat transfer in a combustion chamber when one chooses plume details as independent variables, i.e., by varying values of the constants in the equation.

Even though the in-cylinder species distribution is given, very likely in a coordinate system with respect to the injection nozzle, it is needed to find the species distribution along the optical paths centered at the location of which incident heat flux is sought. Because of its complexity, simplified methods have been employed in previous radiation computations; uses of geometric factors [5,6], zonal method [7], etc. A new coordinate transformation method is introduced for finding an accurate species distribution along each optical path centered at individual locations over the combustion chamber, when the in-cylinder distribution is given with respect to the nozzle hole [8]. A short summary of the method is given here: Referring to Fig. 1 which shows plumes

distributed in a cylindrical coordinate centered at the nozzle hole, R , one wants to find the species distribution along an optical path faced by a particular location on the wall (called a detector for simplicity's sake), D .

A new equation was derived for this purpose as shown in the following (Fig. 1) or for a given property distribution with respect to the nozzle as shown in Eq. (1), the property distribution along an optical path (r, θ, ζ) , s , is expressed as,

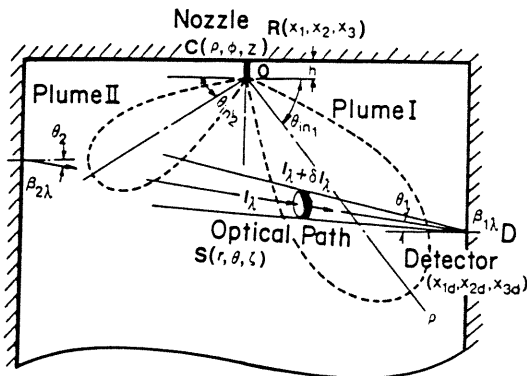


Fig. 1. A Schematics of Flame Plumes in a Combustion Chamber

$$s = s_d e^{-[r-r_c]/r_w]^2} \quad (2)$$

where,

$$s_d = f_v e^{-(a_1 - b_1^2/4c_1)}$$

$$r_c = b_1/2c_1$$

$$r_w = (c_1)^{-1/2}$$

$$a_1 = a\rho_d + b\phi_d + cz_d^2$$

$$b_1 = -[a\rho_1 + b\phi_1] \sin \phi / \rho_d + 2c z_d \cos \theta$$

$$c_1 = [a\rho_2 + b\phi_2] \sin^2 \theta / \rho_d^2 + c \cos^2 \theta \quad \text{and } \rho_i \text{ and } \phi_i \text{ (} i = 0, 1, \text{ and } 2\text{) are second order polynomials expressed by using Taylor's expansion in terms of } x = r \sin \theta / \rho_d, r, \theta, \text{ and the plume angle } \phi_{in} \text{ (refer to Fig. 1).}$$

Upon the determination of the species distribution along the individual optical paths, the radiation heat flux incident on the detector through each path is computed. In order to achieve this, the following two steps have to be taken, i.e., to compute the thermal and optical properties of the species and to implement integration of the equation of radiation by combining all the above results. The computations of optical properties along each path were made by

finding radiation from both soot and gases respectively: Rayleigh-limit expression and the dispersion equation are used for finding the monochromatic volume absorptance of soots [5,9] and the non-gray semiempirical band model proposed by Edwards and Balakrishnan [5,10] is employed for computing gas volume absorption. The summation of radiations from both contributions, $\epsilon_{t,\lambda}$, are made equivalent to $\epsilon_{t,\lambda} = 1 - (1 - \epsilon_{g,\lambda})(1 - \epsilon_{s,\lambda})$, where $\epsilon_{g,\lambda}$ and $\epsilon_{s,\lambda}$ are the spectral emissivity due to the presence of gaseous species and soot, respectively. Notice that the monochromatic property variation is a function of the distance along each optical path. Regarding the equation of radiation heat transfer, the following equation was derived. In reference to Fig. 1, when the distribution of the total volume absorptance, $\kappa_\lambda(r)$, is found, the governing equation of local directional spectral radiation intensity, $I_\lambda(r)$, is written as

$$I_\lambda(r) = \int_r^{r_0} \frac{\kappa_\lambda(r')}{\pi} e_{b\lambda}(r') \exp\left(-\int_r^{r'} \kappa_\lambda(r'') dr''\right) dr'.$$

The heat flux along an optical path of a solid angle (θ, ζ) in the thermal radiation range may be, then, found from

$$q_{\theta\zeta} = \int_0^\infty I_\lambda(0) \cos \theta d\lambda \quad (3)$$

where κ_λ is the spectral volume absorptance at (r, θ, ζ) . Combining Eq. (2) with the above equation, a better implementation of its computation has been made by using Gaussian integration method [11].

Due to the repeated computation of the adiabatic flame temperature based on the local burned fuel/air ratio along the individual optical paths, a convenient way was sought to find the temperature values. A simple form of equation was developed in a direction of its proper coupling with Eq. (3) for facilitating the subsequent solution. The new equation of the adiabatic flame temperature, T_a , is functionally related to several variables, i.e., the fuel volume fraction of stoichiometric, Λ , the reaction pressure p , the initial temperature of mixture, T , and the number of carbon atoms in the fuel, I , as shown in the following [12]:

$$T_a = A_1 [1 + A_2 \Lambda n \Lambda + A_3 (\Lambda n \Lambda)^2] \quad 0.5 < \Lambda \leq 1.0 \quad (4)$$

where A_1 , A_2 and A_3 are functionally expressed in terms of p , T and I . The constants in those expressions for most of practically used fuel/air systems are given in the above reference.

In addition, the spectral surface reflectivity is incorporated with the spectral radiation heat flux incident on each detector over the combustion chamber wall. By defining the extinction coefficient, τ , along the optical path and giving the spectral surface reflectivities, β_1 and β_2 (see Fig. 1), the radiosity of the surface 1, B_1 , is expressed as

$$B_1 = \frac{(I_1 + \beta_{\lambda 1} \cos \theta_1 I_{op}) + \beta_{\lambda 1} \cos \theta_1 e^{-\tau} (I_2 + \beta_{\lambda 2} \cos \theta_2 I_{op})}{1 - \beta_{\lambda 1} \beta_{\lambda 2} \cos \theta_1 \cos \theta_2 e^{-2\tau}} \quad (5)$$

where $I_i = \epsilon_i \sigma T_i^4$ ($i = 1, 2$) and $\beta_{\lambda} = 1 - \epsilon_{\lambda}$.

PARAMETRIC ANALYSIS OF DIESEL RADIATION HEAT TRANSFER

Since the details of instantaneous in-cylinder events are not known due to either the insufficient experimental data or the limitations in combustion modeling, several assumptions are taken in the present computational analysis. The main assumptions are: (1) the system for each computed entity is isolated; (2) the species in the system attains an equilibrium at successive moments; (3) the temperature distribution is that of the adiabatic flame temperature determined by the burned local fuel/air ratio and cylinder pressure; (4) the fuel is injected into the combustion chamber at an inclined angle, $\theta_{in} = 150^\circ$; (5) the scattering in the radiation is negligible; and (6) the standard values of constants for convenience of comparison in Eq. (1) are, f_0 for soot, H_2O , CO_2 and fuel/air ratio, 8×10^{-6} , 0.01, 0.01 and 1.0, respectively. In addition, the distribution constants a , b , and c are 0.6, 2.36 and 2 accordingly. For example, the fuel/air ratio distribution, may be written as $\Lambda = \{1.0 \exp -[0.6(\rho/R) + 2.43(\theta/\theta_r) + 2.0(z/R)^2]\}$, where R is the piston radius and θ_r is π /(the number of plumes). Further, the analysis was made for the following engine details; the surface temperature, $500^\circ K$; number of spray plumes, 4; piston radius, 4.92 cm; combustion chamber bowl radius, 3.44 cm and the fuel composition, $C_{16}H_{34}$.

The computation was carried out to evaluate the following: the apparent emissivity (or normalized radiation heat transfer), $\epsilon_a = q/q_r$; the spectral emissivity (or normalized spectral radiation heat transfer), $\epsilon_{\lambda} = q_{\lambda}/q_{r\lambda}$; the spectral apparent emissivity (or normalized relative spectral radiation heat transfer), $\epsilon_{\lambda a} = q_{\lambda}/q_{r\lambda}$, where $q_r = \sigma T_r^4$, $T_r = 2400^\circ K$; $\lambda_r = 6.0 \mu m$; and $\sigma = 2\pi^5 k^4 / 15c^2 h^3$, $c = 2.998 \times 10^{10}$ cm/sec, $h = 6.625 \times 10^{-27}$ erg-sec, and $k = 1.380 \times 10^{-16}$ erg/K. Additionally, in order to evaluate the effect of the presence of the combustion chamber wall on the radiation, three different computations of heat flux were evaluated (as shown in results): Net, computation of radiation on heat flux through the wall with inclusion of the emission of the spray plumes, the absorption and emission of the wall and the reflection from the surroundings; No Reflection, computation including the emission of the spray plumes plus the absorption and emission of the wall but excluding the reflection and emission from the opposite walls; and Spray Plume, computation of radiation streaming out of the spray plumes only.

The results obtained by using the above conditions and assumptions are shown in the following for various parameters with relevant explanations.

Location of Detector (ρ_d, ϕ_d, z_d). A computation was carried out for heat fluxes through the locations on the cylinder head across a plume at $\rho_d = 0.5$ and along the direction of a plume axis ($\phi_d = 0$) and their results are shown in Figs. 2 and 3 respectively. The trend shows the radiation flux quite similarly follows the species

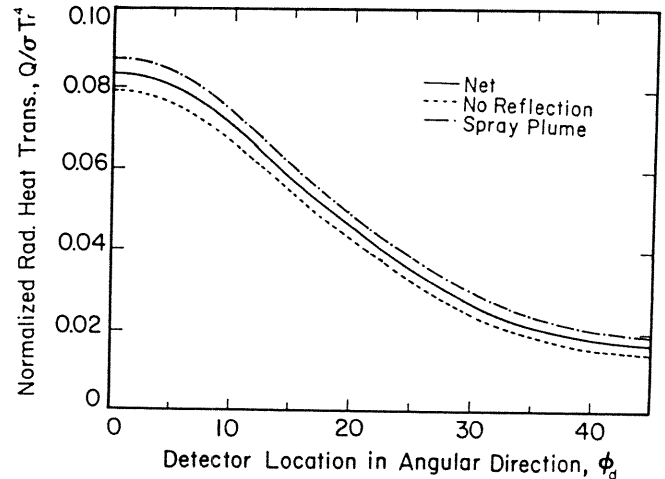


Fig. 2. Radiation Heat Flux Through a Cylinder Wall Along the Axial Direction of a Plume

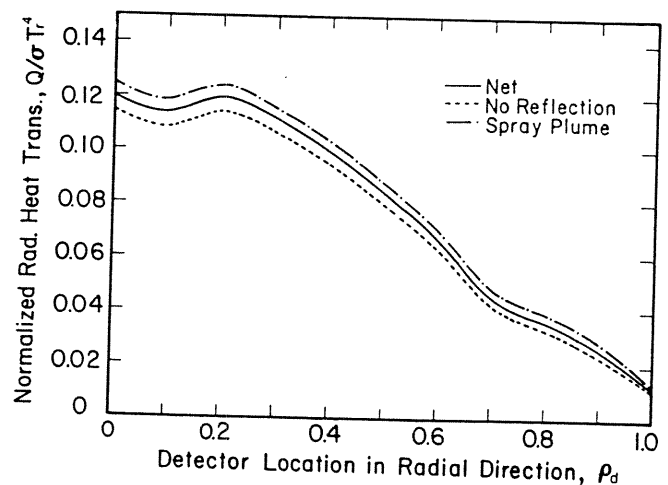


Fig. 3. Radiation Heat Flux Through a Cylinder Wall Along the Circumferential Direction Across a Plume

distribution in the corresponding plume. This suggests the greatest portion of heat flux incident on a detector comes from the radiation source right beneath the detector, as indicated by the directional cosine in Eq. (3). A similar conclusion was made in the authors' preliminary radiation modeling of diesel combustion [5]. The local minimum around $\rho_d = 0.1$ may be of surprise. In order to find its reason, the net directional radiation intensity was calculated at different locations along the axis ($\phi_d = 0$) by varying the azimuthal angle (ϵ) of integration with an azimuth

angle of $\theta = 39.7^\circ$, as shown in Fig. 4: The reason for the minimum at $\rho_d = 0.1$ is readily explained from the figure by finding that while the radiation heat flux incident on the detector at the nozzle ($\rho_d = 0$) is from all of the four plumes, the heat flux on the detector at $\rho_d = 0.1$ is from the species from one plume, i.e., the nearest plume.

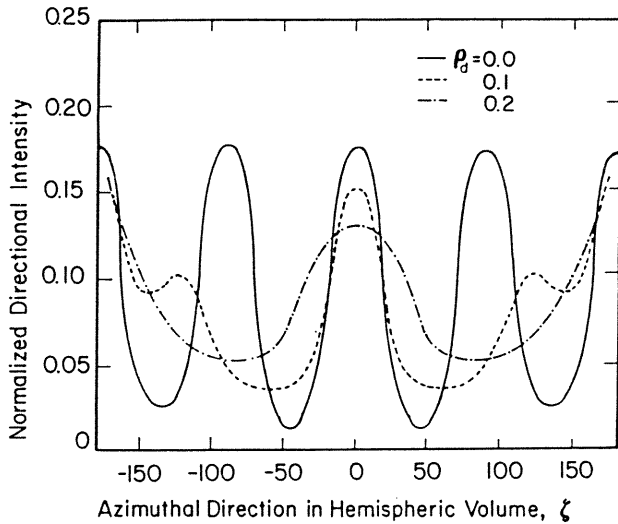


Fig. 4. Net Directional Intensity Incident on Zineith Angle of 39.7° in the Hemispheric Volume (r, θ, ζ) Faced by Detectors Along a Plume Axis

The radiation heat flux incident on the piston surface (with the cup depth of 0.74 cm) for $\phi = 0$ was calculated as shown in Fig. 5. The trend of results is predictable; the local minimum at $\rho_d = 0$ is caused by the weak emission species right underneath the nozzle; the abrupt change around $\rho_d = 0.7$ is due to the presence of the piston bowl bank.

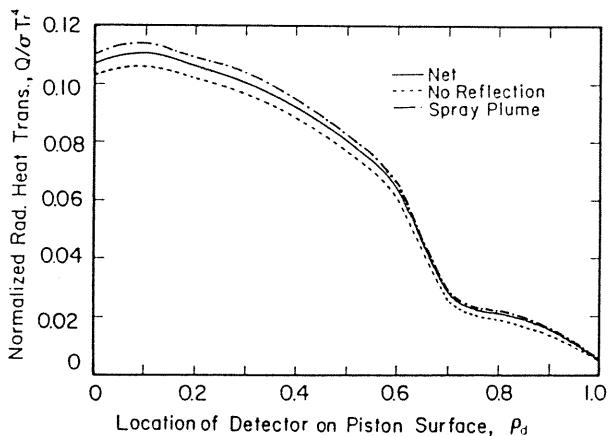


Fig. 5. Radiation Heat Flux Through a Piston Surface Along the Axial Direction of a Plume

A similar computation was conducted for the heat flux incident on the side wall of the piston cup as shown in Fig. 6. The strongest heat flux

was not found for the straight end of the plume ($\phi_d = 0$) but for $\phi_d = 10$. The humps in the curve were found to occur due to the geometric configuration of other plumes from a similar analysis to results in Fig. 4.

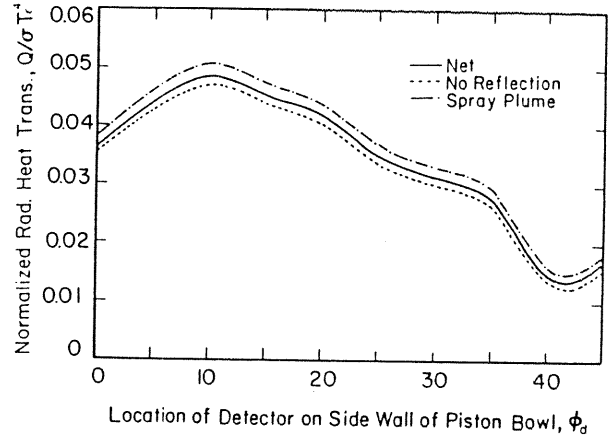


Fig. 6. Radiation Heat Flux Through a Piston-Cup Side Wall

The heat flux on the cylinder liner ($\rho_d = 1$) may be of interest: Computation was made for $z_d = -0.044$ as shown in Fig. 7. The decrease in heat flux with ϕ_d was expected because the species concentration near the detector becomes leaner with increase in ϕ_d . The relatively flat curve between $\phi_d = 10^\circ$ and $\phi_d = 35^\circ$ indicates the increasing effect of the neighboring plume on the heat flux. Note that the heat flux striking the cylinder wall at $\rho_d = 1$ is stronger than that at the similar location on the cylinder head. Also note that the heat flux, in general, is much stronger on the cylinder head (Fig. 3) than the cylinder liner (Fig. 7).

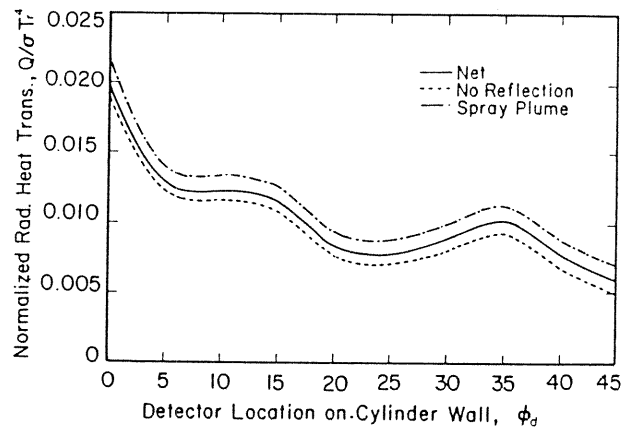


Fig. 7. Radiation Heat Flux Through a Cylinder Liner Along the Circumferential Direction

Surface Emissivity. In Figs. 2 and 3, the energy-spray plume is greatest and the energy-net is greater than the energy-no reflection. This result may be conveniently explained by the following example. At $\rho_d = 0$, since the detection

surface absorbs 95% of the incident energy (with reflection of 5%) and emits an amount of energy ($T_w = 500^\circ\text{K}$) equivalent to 1.4% of radiation energy from the spray plume (q_{sp}), the energy-no reflection is 93.6% of the energy-spray plume. Computational results show the energy-net is 96.8% of q_{sp} ; the difference of the two, 3.2% (96.8%-93.6%) of q_{sp} is, therefore, the energy reflected from the opposite surface walls. Since, from this example, 5% of reflection and 1.4% of emission from the chamber surfaces result in a 3.2% of increment of the energy detected by a location of the chamber, it may be concluded the following: A net energy equivalent to about one half of the energy leaving a surface will arrive at the same surface when incorporated the emission from the opposite wall with the extinction along the optical paths.

The effect of the above trend may be inferred for different surface emissivities from the results shown in Fig. 8. The decrease of heat flux-net with decrease in emissivity is caused by the increase in reflectivity. At the present, the spectral emissivity of the wall is being incorporated into the analysis for further investigation as a continuing activity at Rutgers.

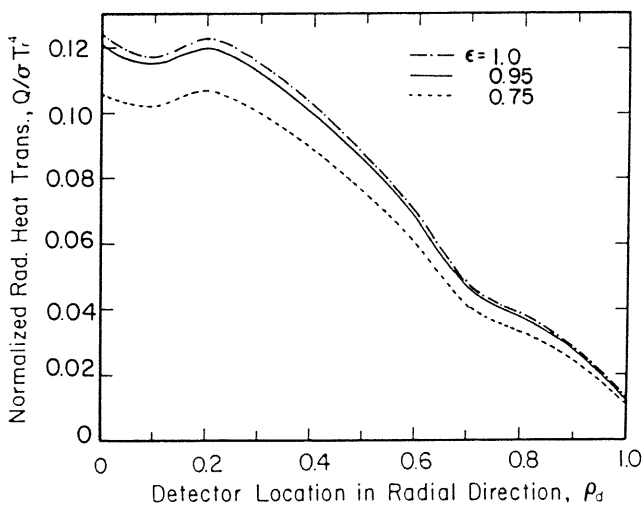


Fig. 8. Effect of Surface Emissivity on Radiation Heat Flux Through a Cylinder Head

Soot Concentration. The radiation heat flux increases with the soot concentration in the plume as shown in Fig. 9. The increase is greater in the lower concentration range than that high concentration. The reason for the convergence of the emissivity at high soot concentration is due to the exponential function relationship of the emissivity to the volume absorptance. Another look at Fig. 9 will lead one to find the local minimum in heat flux does not occur for low soot concentrations. The result is more evidence to explain the unique receiving geometric configuration at the injection nozzle for some cases.

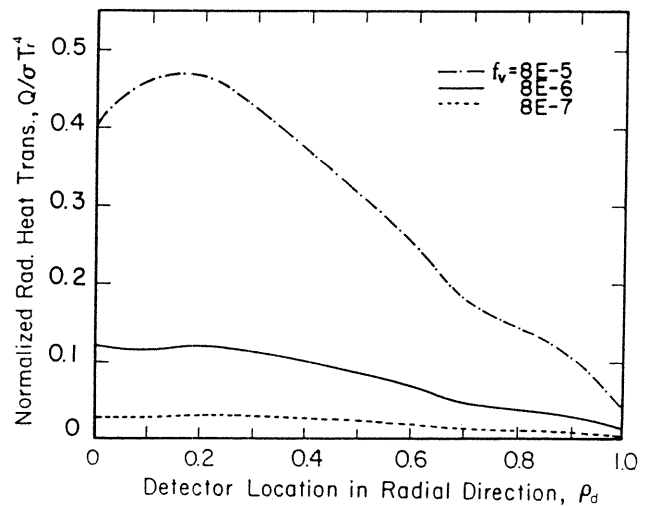


Fig. 9. Soot Concentration Variation Effect on Radiation Heat Flux Through a Cylinder Head

Soot and Gas Radiation. As expected from the authors' previous study [5], it is found that the soot radiation is much stronger than the gas radiation (Fig. 10). The direct summation of soot radiation and gas radiation exceeds the computed combined radiation. While its reason may be explained by looking into the method of combination [4,8], it can also be seen from the fact that some gas emission is absorbed by soots and that soot radiation is similarly attenuated by the presence of the gas species.

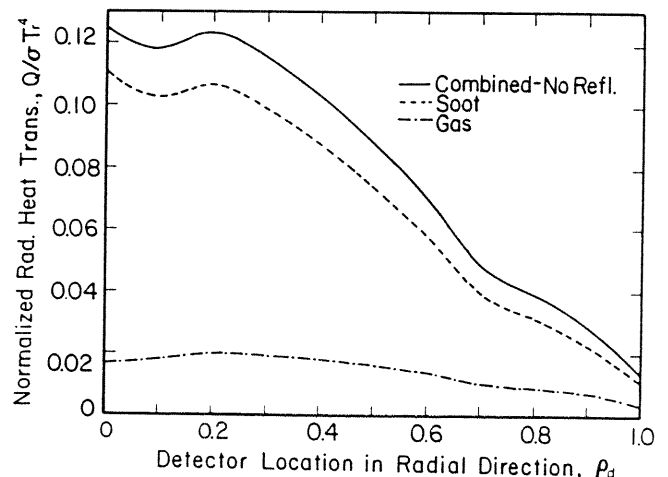


Fig. 10. Comparison of Radiation Heat Fluxes Due to Soot and Gaseous Species

In order to investigate predominant wave bands of radiation, a wave number-resolved computation was made as shown in Fig. 11. There are three distinctively strong bands of gas radiations at $\lambda = 1, 3$ and $10 \mu\text{m}$ (recall that the normalized wave number = $\lambda/6 \mu$). In fact, each band consists of many small bands of CO_2 and H_2O in the plume. Over the spectra of radiation, one finds that soot radiation is dominant in short wavelength, $\lambda < 2 \mu\text{m}$, while the gas radiation

becomes important in longer wavelengths, $\lambda > 4 \mu\text{m}$ (Fig. 12).

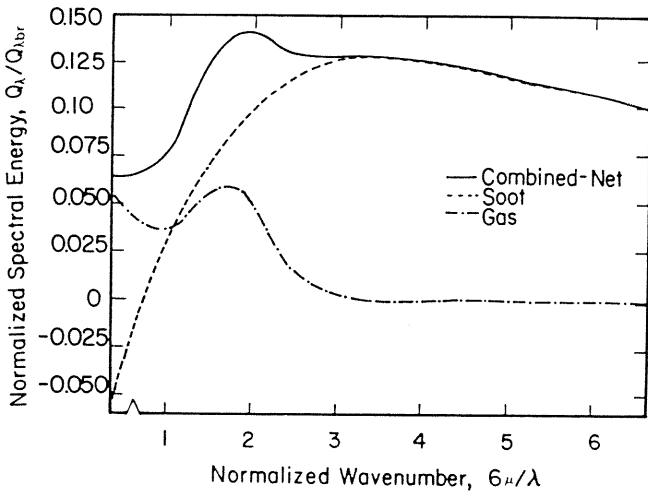


Fig. 11. Spectral Radiation Heat Flux Due to Soot and Gaseous Species

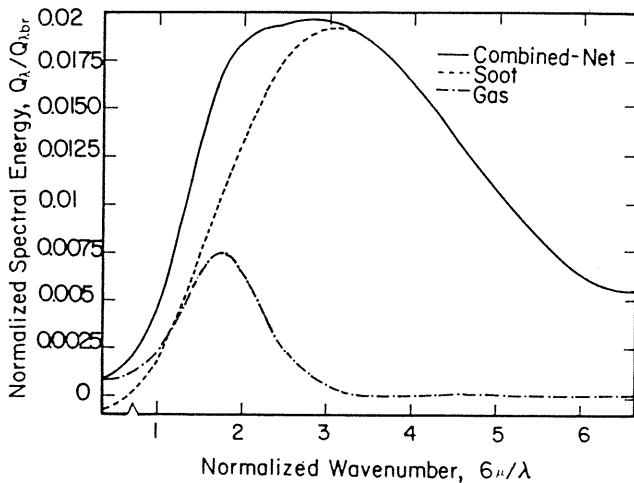


Fig. 12. Relative Spectral Radiation Heat Flux Due to Soot and Gaseous Species

Pressure. The effect of pressure on radiation heat transfer was studied assuming the injection processes and the gas motions are not affected. Figure 13 shows the computational results of the pressure effect on spectrum-resolved radiation heat flux at $\rho_d = 0$. The variation of the spectral radiation with pressure is somewhat noticeable at the long wavelength region ($\lambda > 3 \mu\text{m}$) where the gas radiation is important. Since the flame temperature is relatively insensitive to the pressure variation, the results in Fig. 13 only show the pressure broadening effect on the gas radiation in diesel combustion.

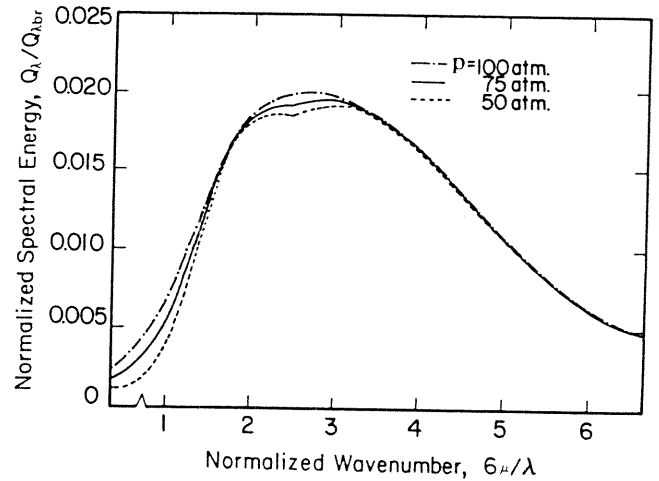


Fig. 13. Pressure Broadening Effect on Diesel Radiation Heat Transfer

Surface Temperature. The weak effect of the chamber surface temperature variation on the radiation heat transfer is shown in Fig. 14. There is some reduction in the energy-net due to the stronger surface emission at higher surface temperature. Such an effect will be greatly increased in some local places where the surface temperature, however, is extremely high in the engine combustion chamber.

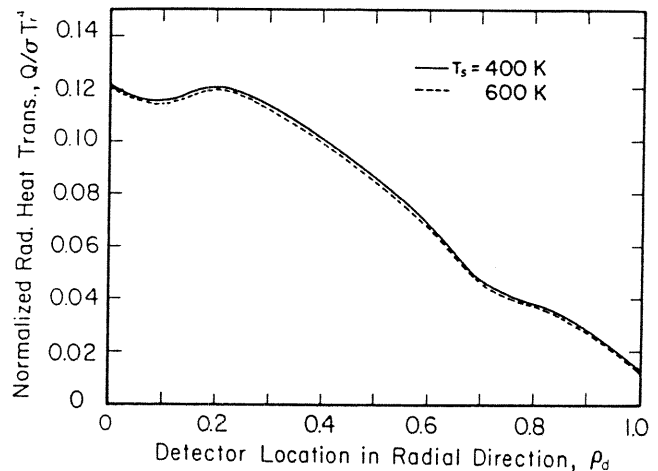


Fig. 14. Surface Temperature Effect on Diesel Radiation Heat Transfer

Burned Fuel/Air Ratio vs. Soot Concentration vs. Flame Temperature. In order to mutually compare parameters greatly affecting the radiation heat transfer, Figs. 14, 15 and 16 are offered. Several important points found from the results may be in order: the effect on the radiation heat transfer is much greater with the relative variation of the fuel/air ratio than that of the soot concentration. The greater effect of the fuel/air variation is caused by the corresponding changes in CO_2 and H_2O concentrations and the adiabatic flame temperature. Note that the temperature effect on volume absorptance is the quadruple power dependency of temperature and the soot concentration effect on it is the linear

relationship of soot concentration.

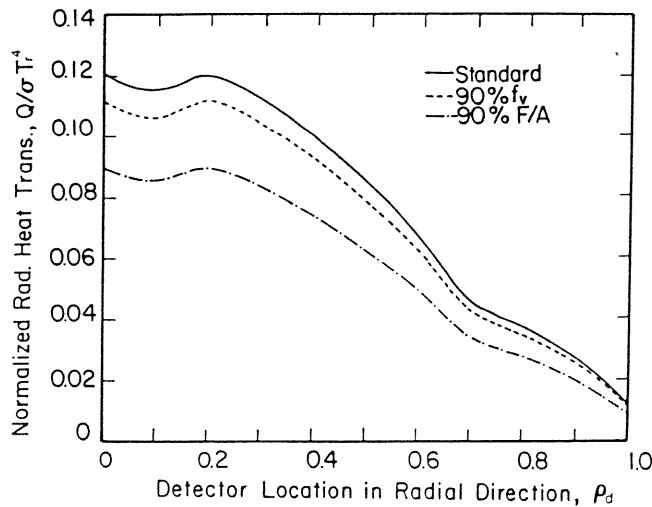


Fig. 15. Comparison of Effects on Diesel Radiation Heat Transfer Due to Variations in the Soot Concentration and the Fuel/Air Ratio

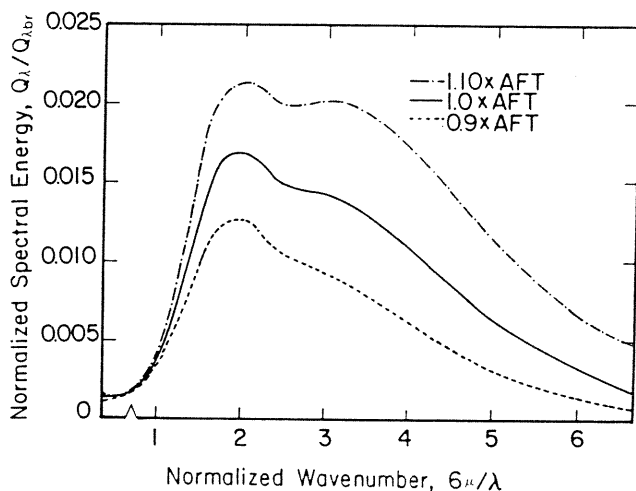


Fig. 16. Comparison of Effects on Relative Spectral Radiation Heat Transfer Due to Variations in the Soot Concentration and the Fuel/Air Ratio

Since the adiabatic flame temperature is not realistic, at all, in diesel combustion, the sensitivity of radiation heat transfer to the temperature variation is worth investigating. Note that the actual flame temperature in diesel combustion may either higher or lower than the adiabatic flame temperature due to the post-reaction compression, heat transfer, etc. Figure 15 shows the effect of temperature on the radiation heat flux. Note that there is an assumption of no change in gaseous species concentrations in this variation, unlike in the fuel/air ratio variation. As mentioned above, because of the quadruple dependence of temperature on the volume absorptance and due to the weak effect of the variation in gaseous species concentrations on the radiation, the impact of

temperature variation on the process is concluded to be very high as shown in the results. Figure 16 shows the stronger effect of the temperature variation on the radiation heat transfer at shorter wavelengths. This may be well explained by Planck's radiation function.

SUMMARY

A new radiation heat transfer model of direct injection diesel combustion has been developed. The model has been used for a parametric analysis of radiation transmission in a diesel engine. Some of the results may be misleading due to the lack of sufficient combustion details of the engine. Nevertheless, the present results clearly show that the engine radiation processes may be well analyzed by using the new model and that some new findings are worth noting:

(1) The most portion of radiation heat flux incident on a location in the chamber wall comes from the radiation source right near the location.

(2) The effect of surface emissivity on diesel radiation may not be negligible, in particular, when the surface temperature is high, as in new uncooled diesel engines.

(3) The diesel radiation heat transfer is highly dependent on the soot concentration and weakly sensitive to the gaseous species concentrations.

(4) The pressure effect on the radiation is almost negligible in diesel combustion.

(5) The surface temperature of the chamber wall is not a sensitive parameter on the diesel radiation heat transfer, but it will not be negligible where the local temperature is exceedingly high.

(6) The flame temperature or the fuel/air ratio variation produces very high impact on the radiation process, more than any other parameter studied.

ACKNOWLEDGEMENT

The present study has been supported by the U.S. Army Research Office, Contract No. DAAG29-83-K-0042 (Scientific Program Officer, Dr. David M. Mann).

NOMENCLATURE

a	species distribution constant
A	constants in adiabatic flame temperature equation
b	species distribution constant
B	radiosity of surface
c	speed of light
f	species distribution with respect to injection nozzle
f ₀	species distribution constant
f _v	soot volume fraction
h	Planck's constant
I	radiation intensity or number of carbon atoms in a fuel

k	Boltzmann constant
p	pressure
q	radiation heat flux
r	optical path
R	radius of cylinder
s	species distribution with respect to detector
T	temperature
ρ, ϕ, z	components in cylindrical coordinate
r, θ, ζ	components in spherical coordinate
β	surface emissivity
κ	volume absorptance
λ	wavelength
Λ	fuel volume fraction of stoichiometric
τ	extinction coefficient
σ	Stefan-Boltzman constant

Subscripts

a	adiabatic
b	blackbody
d	detector
g	gas
i	index number
op	optical path
r	reference
s	soot
t	total
λ	spectral

REFERENCES

- Ahn, S.K., Matsui, Y., Kamimoto, T. and Matsuoka, S., "Measurement of Flame Temperature Distribution in a D.I. Diesel Engine by Means of Image Analysis of Nega-Color Photographs," SAE Paper-810183, 1981.
- Aoyagi, Y., Kamimoto, T., Matsui, Y. and Matsuoka, S., "A Gas Sampling Study on the Formation Processes of Soot and NO in a D.I. Diesel Engine," SAE Paper-800254, 1980.
- Rhee, K.T., Myers, P.S. and Uyehara, O.A., "Time- and Space-resolved Species Determination in Diesel Combustion Using Continuous Flow Gas Sampling," SAE Paper-780226, 1978.
- Chang, S.L. and Rhee, K.T., "An Analytical and Numerical Modeling of Radiation Heat Transfer in Combustor Having Jet Flames," 4th International Conference on Applied Numerical Modeling, December 27-29, 1984, Taiwan.
- Chang, S.L. and Rhee, K.T., "Computation of Radiation Heat Transfer in Diesel Combustion," SAE Paper-831332, 1983.
- Chapman, M., Friedman, M.C. and Aghan, A., "A Time-Dependent Spatial Model for Radiant Heat Transfer in Diesel Engines," SAE Paper-831725, 1983.
- Menguc, M.P., Viscanta, R. and Ferguson, C.R., "Multidimensional Modeling of Radiative Heat Transfer in Diesel Engines," SAE Paper-850503, 1985.
- Chang, S.L. and Rhee, K.T., "Coordinate Transformation Method for Radiation Heat Transfer Prediction in Soot Laden Combustion Products," to be published.
- Dalzell, W.H. and Sarofim, A.F., "Optical Constants of Soot and their Application to Heat Flux Calculation," Trans. of ASME, Vol. 9, p. 100, 1969.
- Edwards, D.K. and Balakrishnan, A., "Thermal Radiation by Combustion Gases," International Journal of Heat Mass Transfer, Vol. 16, p. 25, 1973.
- Chang, S.L. and Rhee, K.T., "A Solution of Radiation Heat Transfer Equation in Combustors with Plumes Consisted of Radiatively Participating Species Distribution," being prepared.
- Rhee, K.T. and Chang, S.L., "Empirical Equations for Adiabatic Flame Temperatures for Some Fuel-Air Combustion Systems," Combustion Science and Technology, Vol. 44, 75, 1985.